Journal of Groundwater Science and Engineering
ISSN 2305-7068
Indexed by ESCI CABI CSA Scopus GeoRef AJ CNKI

Presenting and evaluating a new empirical relationship for estimating the rate of infiltration in trenches

Mojtaba Hassanpour, Hossein Khozeymehnezhad, Abalfazl Akbarpour

Citation:
Hassanpour M, Khozeymehnezhad H, Akbarpour A. 2025. Presenting and evaluating a new empirical relationship for estimating the rate of infiltration in trenches. Journal of Groundwater Science and Engineering, 13(2): 101-115.

View online: https://doi.org/10.26599/JGSE.2025.9280042

Journal homepage: http://gwse.iheg.org.cn

Presenting and evaluating a new empirical relationship for estimating the rate of infiltration in trenches

Mojtaba Hassanpour[1], Hossein Khozeymehnezhad[1*], Abalfazl Akbarpour[1]

[1] *University of Birjand, Birjand* 9717434765, *South Khorasan, Iran.*

Abstract: Empirical formulas are indispensable tools in water engineering and hydraulic structure design. Derived from meticulous field observations, experiments, and diverse datasets, these formulas help to estimate water leakage in structures such as dams, tunnels, canals, and pipelines. By utilizing a few easily measurable parameters, engineers can employ these formulas to generate preliminary leakage rate estimates before proceeding with more detailed analyses. In this study, a physical model was developed, and a series of experiments were conducted, considering variables such as inflow rate, materials constituting the unsaturated medium, and variations in infiltration trench depth and width. As a result, a novel artificial recharge method was introduced, and an empirical equation, $Q_{out}= 0.0066 \times D_{50}^{0.64} \times L \times P^{0.36}$, was proposed to estimate the infiltration capacity of the trench. This equation incorporates factors such as the wetted perimeter, mean soil particle diameter, trench length, and a coefficient. A comparative analysis between the observed data from nine Iranian earthen canals and the values calculated using the proposed equation revealed an average relative error of 15% between the two datasets. In addition, the Pearson correlation coefficient was determined to be 0.981 and the Root Mean Square Error (RMSE) was 0.381, demonstrating the strong predictive performance of the equation. The parameters considered in the proposed equation allow for its application across diverse regions. Given its accurate performance, this equation provides a reliable initial estimate of the leakage rate, thereby helping to reduce costs and save time.

Keywords: Groundwater; Artificial recharge; Desert area; Infiltration rate; Physical model

Received: 12 May 2024/ Accepted: 21 Oct 2024/ Published: 10 May 2025

Introduction

The growing global demand for water resources, particularly in arid and semi-arid regions, has highlighted the need for innovative approaches to water storage and reuse. This has prompted extensive research into new methods for effectively utilizing groundwater and surface water (Karim, 2018). In arid and semi-arid regions, surface water sources are often limited and unpredictable, making groundwater the primary source of water (Scanlon et al. 2006; Li et al. 2021). Various water resources can be utilized in the artificial feeding process, including rainwater, seasonal and permanent rivers, natural water reservoirs like lakes and wetlands, water from alternate water tables, sewage, agricultural runoff, and water leakage from water supply networks, among others (Senent-Alonso, 1984; Murillo-Díaz, 2004). Depending on the type of water source, artificial feeding can be implemented through surface methods such as ponds, channels, and dams, or subsurface methods like absorption wells and radial drains. It is worth noting that surface methods are generally considered more expensive (Foreman, 2014). Managed Aquifer Recharge (MAR) offers a promising solution for addressing groundwater resource issues, allowing excess surface water to be stored underground for future use. For example, the Pliocene sand and gravel (Crag) aquifer in Suffolk, UK, was selected for a demonstration MAR scheme due to its favorable hydrogeological characteristics, with the aim of supplying additional irrigation water during the summer months (Hiscock et al. 2024).

*Corresponding author: Hossein Khozeymehnezhad, *E-mail address*: Hkhozeymeh@birjand.ac.ir

DOI: 10.26599/JGSE.2025.9280042

Hassanpour M, Khozeymehnezhad H, Akbarpour A. 2025. Presenting and evaluating a new empirical relationship for estimating the rate of infiltration in trenches. Journal of Groundwater Science and Engineering, 13(2): 101-115.

In arid and semi-arid zones, water is the most vulnerable resource to climate change. To address this vulnerability, various techniques such as artificial recharge are adopted to restore aquifers and ensure their sustainability in response to the accelerated exploitation rates (Lhassan et al. 2019). Several countries, recognizing this issue, have implemented advanced techniques such as artificial recharge to enhance groundwater potential. This technique employs unconventional re-sources, such as floodwater (El Mansouri and El Mezouary, 2015), treated wastewater, and desalinized seawater or demineralized brackish water. These water resources can be collected and used during periods of deficit (Detay and Bersillon, 1996; Rognon, 2000; Pyne, 2005), contributing to aquifer recharge and raising the water table.

However, one challenge associated with artificial recharge is clogging, which involves complex chemical, physical and biological physical processes (Nan et al. 2016). Artificial recharge is widely practiced in regions with excessive aquifer drawdowns to increase groundwater potential (Sebbar, 2013). The simulation of flow in porous media has broad applications, including designing rock dams, sand filters, and optimizing the use of underground water sources. Over the past century, numerous efforts have been made to simulate flow in porous media using Darcy's law and non-Darcy's laws. These simulations have been crucial in understanding and predicting fluid behavior in porous media systems (Afzali et al. 2009).

In groundwater analysis, it is often assumed that horizontal permeability is greater than vertical permeability (especially for clays). The heterogeneity of permeability is quantified by the dimensionless parameter r_k, which is the ratio of horizontal permeability to vertical permeability ($r_k=k_h/k_v$). Among many values of r_k are available for clays and rocks, valid results for non-cohesive materials are scarce due to limited permeability measurement devices for granular materials (Bagarello et al. 2009).

To design an appropriate artificial recharge method, it is essential to gather sufficient information on water flow distribution within the soil. This helps determine the inflow intensity and maximizing the infiltration rate. Soil permeability is influenced by two main factors, the intrinsic characteristics of the soil (such as soil porosity, surface roughness of solid particles, and degree of saturation), and the characteristics of the fluid (water) passing through the soil (Pishro et al. 2017).

Numerous methods have been introduced to quantify and estimate seepage and infiltration in canals, which can be broadly categorized into direct and indirect methods. Direct methods include various field methods (in-flow-out-flow method, ponding method, seepage meter), while indirect methods are based on empirical relationships, such as Ingham, Davis-Wilson, Moritz, India, Molsors and Yenidomiya, Afangenden, as well as analytical and inferential methods (Ali, 2011). While direct methods are more practical and accurate, they require more time and resources. Indirect methods, on the other hand, face criticism due to the assumption of homogeneous natural conditions, which is rarely found in nature. However, they can still provide quantitative predictions of seepage losses (Moghazi and Ismail, 1997).

Empirical relationships for estimating seepage from canals have been developed based on field tests under various conditions (Cui et al. 2004). Due to the regional specificity of coefficients in these empirical equations, they require calibration for accurate application in each location (Salemi and Sepaskhah, 2006). In anisotropic soils, vertical saturated hydraulic conductivity (k_v) differs from horizontal saturated hydraulic conductivity (k_h) (Beckwith et al. 2003). As porosity increases, permeability coefficients rise in both horizontal and vertical directions, with horizontal permeability often being higher (Pishro et al. 2017).

The empirical equation was applied to calculate the leakage ratios of the Golumd, Tatalin, and Iqe Rivers. The results demonstrated a strong correlation with measured leakage quantities, suggesting the equation's reliability and applicability in this specific context. Further analysis involved calculating leakage ratios and quantities for various rivers within the Qaidam Basin. Rivers with flow rates exceeding 10 m^3/s exhibited leakage ratios between 61.1% and 78.3%, while those with flow rates below 5 m^3/s displayed significantly higher leakage ratios of 94.5% to 99.9%. These findings align with the general trend of river leakage in the region. The developed leakage ratio equation offers a valuable tool for estimating leakage in areas with similar hydrogeological characteristics (Zhang et al. 2015).

A study of nine earthen channels in the Isfahan watershed, varying in texture (heavy, medium and light) and vegetation cover (low, medium and high), was carried out using the outflow method. The empirical leakage equations were calibrated and validated (Ingham, Davis-Wilson, Afangenden, Roche Moritz, Molsor and Yanidomia, Misra and Hand) and linear regression equations were established between the measured and calculated leakage values (Salemi and Sepaskhah, 2006). An accuracy assessment of the empirical equations of Ingham, Moritz, Davis-Wilson, Molsource, Yenidomia, and Misra compared to the pond method across three channels in the Qazvin Plain revealed that Misra and Morits methods had the most reliable results. These methods are recommended for estimating leakage in that region (Nouri Mohammadieh et al. 2009).

Further, using water leakage data from nine earthen canals, a comparison between two leakage estimation methods (Ingham and Wedernikow Equation), it was found that the recalibrated Wardnik equation better estimates water leakage from the canals of Rudasht region (Heidarizadeh and Salemi, 2014). The SEEP/W model also performed well in estimating water leakage from seven class 3 and 4 earthen channels downstream of Zayandeh Rood Dam. Comparison with different empirical methods showed that while experimental methods are useful, local recalibration is necessary for precise results (Rastamian and Abdi Koupai, 2012).

In previous studies, seepage rates calculated using empirical equations have typically been compared with measured seepage values from canals. However, only a few studies, such as that by Salemi and Sepaskhah (2006), have undertaken the calibration of the coefficients in these equations. This lack of calibration, particularly for empirical equations designed for specific regional conditions, represents a significant limitation in most of the studies reviewed.

Additonally, conducting seepage estimation tests at the canal site is both time-consuming and costly, further complicating the research process. To address these challenges, physical modeling offers a practical alternative by conducting experiments in controlled laboratory conditions.

Empirical formulas play a vital role in water engineering and hydraulic structures. These formulas, derived from field observations, tests and various experimental data, are commonly used to estimate water leakage from structures such as dams, tunnels, canals and pipelines. They allow engineers to make a preliminary estimate of leakage rates using a few easily calculable parameters before performing more detailed calculations.

When designing effective artificial recharge systems, it is crucial to understand how water flows through soil. This information is key to selecting the right water flow method and maximizing the infiltration rate. Investigating water flow distribution in porous media and developing an efficient artificial recharge system without physical modeling can be both time-consuming and costly. Due to the difficulty of replicating identical in multiple filed-scale experiments, physical modeling was often used. On the other hand, several factors influence the efficiency of artificial recharge method, laboratory limitations often necessitate keeping some variables fixed. Therefore, numerous experiments were conducted to develop an empirical equation aimed at determining the infiltration capacity of a system combining infiltration trench and permeable pipe.

1 Materials and methods

To achieve the objectives in this research, a physical model was constructed in the hydraulic laboratory at the University of Birjand. The model design was inspired by the traditional qanat systems and drainage pipes. Unlike the qanat system, where water is drained from higher elevations down to the qanat canals, this method employs a reverse mechanism. Here, water flows into the permeable pipe and infiltrates downward into the soil layers beneath the pipe region, facilitating artificial groundwater recharge.

Several factors influence the amount of water that exist the model, including the inflow rate, model dimensions, the distance from the bottom of the trench to the water table, soil texture, trench length and width, the height of the overflow pipe relative to the bottom of the trench, and average diameter of the permeable material used. During the experiments, the inflow rate was determined specifically for each soil type used in the initial trials. The width of the infiltration trench, the height of the overflow pipe to the bottom of the trench (trench depth), and the number and arrangement of openings on the variable pipe, and other fixed factors were taken into account.

For this purpose, the model was constructed using 10 mm thick glass, with overall dimensions of 80 cm × 80 cm × 100 cm (Fig. 1). Initially, soil was carefully placed in layers within the model chamber.

Two types of well-graded sand were utilized as separate unsaturated media: Medium sand with D_{50}= 0.74 mm and fine sand with D_{50}= 0.16 mm.

Next, a trench of appropriate dimensions was excavated in the porous medium and filled with high permeability materials, with particle size ranging from 6 mm to 12 mm, to the desired depth. A permeable pipe was then installed within the trench, and a drainage system was installed on top of the trench to remove excess water. Water was

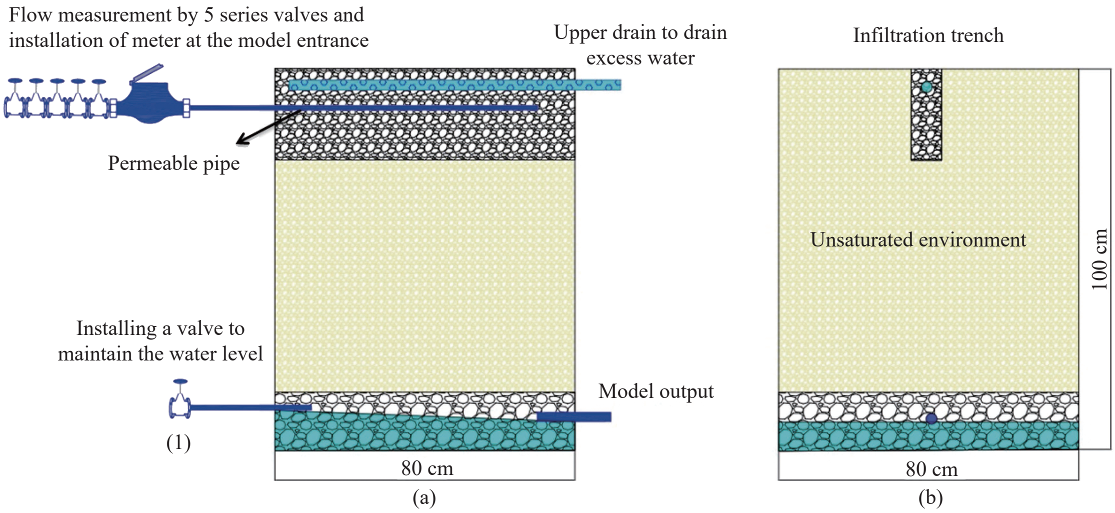

Fig. 1 A simple schematic of the laboratory model

(a) Side view from the right; (b) Front view

supplied to the system through a pipe connected to the municipal water network. On the permeable pipe, six holes with a diameter of 2 mm were created, spaced 15 cm apart. Flow rate measurements were taken using five series valves that had been calibrated in advance using the volumetric method. In addition to flow rate measurement with calibrated valves, the total volume of water passing through the system was also recorded using a water meter.

In the experiments, water flowed through the permeable pipe and trench at a rate of 2.2 liters per minute for the physical model with medium sand materials, and 0.82 liters per minute for the model with fine sand. These input flow rate were established based on the results from preliminary tests.

In the initial phase of the experiments, water was introduced into the trench at these specified flow rates: 2.2 liters per minute for the medium sand and 0.82 liters per minute for the fine sand. The trench dimensions were fixed at a depth of 10 cm, a width of 8 cm, and a length of 80 cm, with the trench length remaining constant in all experiments. The volume of water discharged from the model was recorded.

In the subsequent phase, while maintaining the trench depth, the trench width was varied at ratios of 0.5, 0.75, 1.25, and 1.5 times the initial width. The volume of water discharged from the model was measured for different widths. Additionally, with the width of the trench fixed, the depth was adjusted in the same specified ratios.

Throughout the experiment, water was supplied to the model from point 1 to create and simulate the stagnation level (base flow rate of the model), allowing for more accurate measurement of the output flow rates (Fig. 1a). The municipal water network served as the water source, and a pressure gauge was continuously monitored to maintain stable pressure in the system.

At the start of the experiment, water entered the model at the specified flow rates, and the advancement of the moisture front was recorded every 5 minutes. This process continued until the moisture front reached the water level (Fig. 2a and Fig. 3a).

The moisture front lines were delineated using Plot Digitizer and AutoCAD software. (Fig. 2b and Fig. 3b).

Once the water reached the steady-state level, the output flow rate was measured for all input flow rates of the model. These measurements were taken at 5-minute intervals for duration of 90 minutes, a fixed period determined based on reaching the peak output flow rate from the model and preliminary tests conducted for the minimum flow rate. The maximum output flow rate (Q_{outmax}) was recorded during this stage.

Subsequently, the inlet flow was discontinued, and the output flow rate from the model was measured at 5-minute intervals for an additional 120 minutes. The output flow rate was measured without calculating the base flow rate (Q_{out}) (Equation 1).

$$Q_{out} = (Q_2 - Q_1) \tag{1}$$

Where: Q_1 represents the inlet water flow used to simulate the static level (base flow), and Q_2 represents the output water flow from the model, which includes the inlet water flow used to simulate the static level.

It should be noted that changing the number and arrangement of the apertures while maintaining a consistent total cross-sectional area across all cases

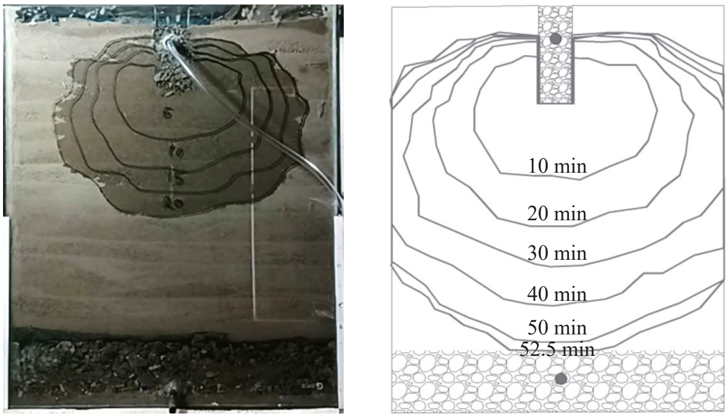

(a) (b)

Fig. 2 How the moisture front moves with 5-minute intervals on the model wall with a trench width of 8 cm and a trench depth of 10 cm (using medium sand materials)

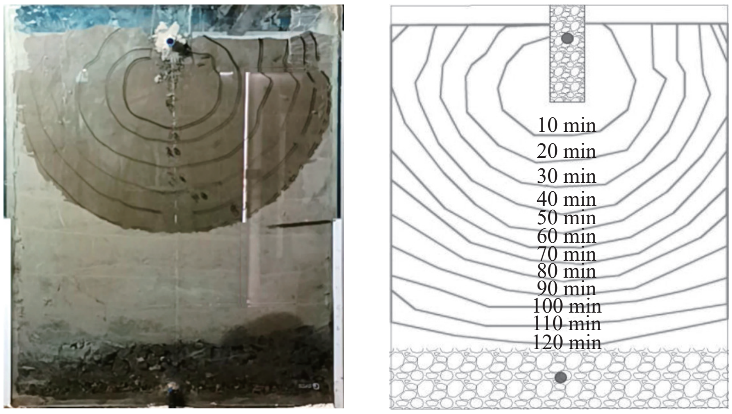

(a) (b)

Fig. 3 Illustration of the moisture front movement in the model wall with 5-minute intervals and a trench width of 8 cm and a trench depth of 10 cm (using fine sand materials)

did not lead to a significant change in Q_{outmax}.

2 Results

2.1 Effect of trench dimensions and sand particle size on flow

The data collected from the experiments is presented in Table 1. In the first row of Table 1, the characteristics of the initial trench for medium sand and fine sand materials are provided. For a constant trench width of 8 centimeters (rows 2 to 5), the volumes of the trench were calculated for depth ratios of 0.5, 0.75, 1.25, and 1.5 relative to the initial trench depth. Similarly, for a constant trench depth of 10 centimeters (rows 6 to 9), the volumes of the trench were calculated for width ratios of 0.5, 0.75, 1.25, and 1.5 relative to the initial trench width.

As observed, the calculated volumes are equal when applying the same ratios for depth and width (Column 4 of Table 1). For example, the calculated volume of the trench in rows 2 and 6 is 3,200 cubic centimeters for a depth ratio of 0.5 and a constant trench width, as well as for a width ratio of 0.5 and a constant trench depth. As indicated by the information in the table 1, for equal trench volumes for both materials, the maximum Q_{out} occurs when the depth-to-width ratio is higher.

In Fig. 4(a) and Fig. 4(c), dimensionless diagrams are shown for different trench depths of 5, 5.7, 10, 5.12, and 15 centimeters, with a constant trench width of 8 centimeters. The input flow rates are 2.2 liters per minute for medium sand materials and 0.82 liters per minute for fine sand materials.

In Fig. 4(b) and Fig. 4(d), dimensionless diagrams are shown for different trench widths of 4, 6, 8, 10, and 12 centimeters, with a constant trench depth of 10 centimeters. The input flow rates are 2.2 liters per minute for medium sand materials and 0.82 liters per minute for fine sand materials:

Q_{out} represents the output flow rate from the

Table 1 Data obtained from the experiments conducted on the physical model with medium sand and fine sand materials

Row	Trench width /cm	Trench depth /cm	Trench volume /cm^3	The ratio of the depth to the width of the trench	Q_{outmax} (Lit/Min) (Medium sand)	Q_{outmax} (Lit/Min) (Fine sand)	Performance (Medium sand) (Q_{out} to Q_{in})	Performance (Fine sand) (Q_{out} to Q_{in})
1	8	10	6,400	1.25	1.990	0.740	0.905	0.902
2	8	5	3,200	0.63	1.820	0.640	0.827	0.780
3	8	7.5	4,800	0.94	1.930	0.688	0.877	0.839
4	8	12.5	8,000	1.56	2.050	0.775	0.932	0.945
5	8	15	9,600	1.88	2.140	0.810	0.973	0.988
6	4	10	3,200	2.5	1.960	0.690	0.891	0.841
7	6	10	4,800	1.67	1.980	0.720	0.900	0.878
8	10	10	8,000	1	2.010	0.752	0.914	0.917
9	12	10	9,600	0.83	2.030	0.770	0.923	0.939

physical model.

Q_{out_R} represents the output flow rate from the physical model considering the initial dimensions of the trench (depth of 10 centimeters and width of 8 centimeters).

t_{Total} represents the total experiment time.

$t_{Q_{in}}$ represents the time from the moment water exits the outlet of the physical model until the input flow is cut off.

The ascending branch of the diagrams shows the period from the moment water exits the model until Q_{outmax} occurs. After reaching the peak of the diagram, Q_{outmax} continues until the end of the constant time designated for all experiments. The descending branch of the diagram represents Q_{out} after the cessation of Q_{in}, which decreases over time.

2.2 Relationship between trench volume, Wetted area, and flow output

Several insights can be drawn from Fig. 4. First, increasing the depth has a significant impact on the seepage rate compared to increasing the width. Additionally, the increase in seepage area leads to a more pronounced rise in the seepage rate for fine sand compared to medium sand. However, the relationship between the increase in seepage rate and the infiltration area is not consistent. For example, as seen in rows 2 and 5 of Table 1, a 2.11-fold increase in the infiltration area (wetted perimeter) results in only 1.26-fold increase in seepage rate.

Figs. 5 and 6 illustrate the variations in trench volume, wetted area, and outflow discharge based on alterations in both trench width and depth for both medium and fine sand types. The horizontal axis in each graph represents the test number, arranged according to the increasing trench volume or area, while the vertical axis indicates the dimensionless ratio of each test to the initial test.

By increasing the volume and wetted surface area of the trench, the output flow rate increases in both medium sand and fine sand conditions. However, it should be noted that the slope of changes in trench volume and wetted surface area is not proportional to the slope of output flow changes and shows a higher value. The slope of trench volume changes was calculated to be 20% based on depth and width changes. Additionally, the slope of changes in the wetted surface area of the trench was calculated to be 14.3% for changes in depth, while the slope for changes in width was calculated as 5.7%. Simultaneously, the slope of the outflow changes corresponding to trench depth changes was found to be 2.8% for medium sand and 4.6% for fine sand. Conversely, the slope of output flow changes associated with variations in trench width was calculated to be 0.8% for medium sand and 2.2% for fine sand.

2.3 Presenting the empirical equation

Using the data obtained from the experiments and investigating the effects of the wetted environment and the average diameter of the soil particles, the experimental equation was derived using nonlinear regression (Equation (2)).

$$Q_{out} = 0.0066 \times D_{50}^{0.64} \times L \times P^{0.36} \tag{2}$$

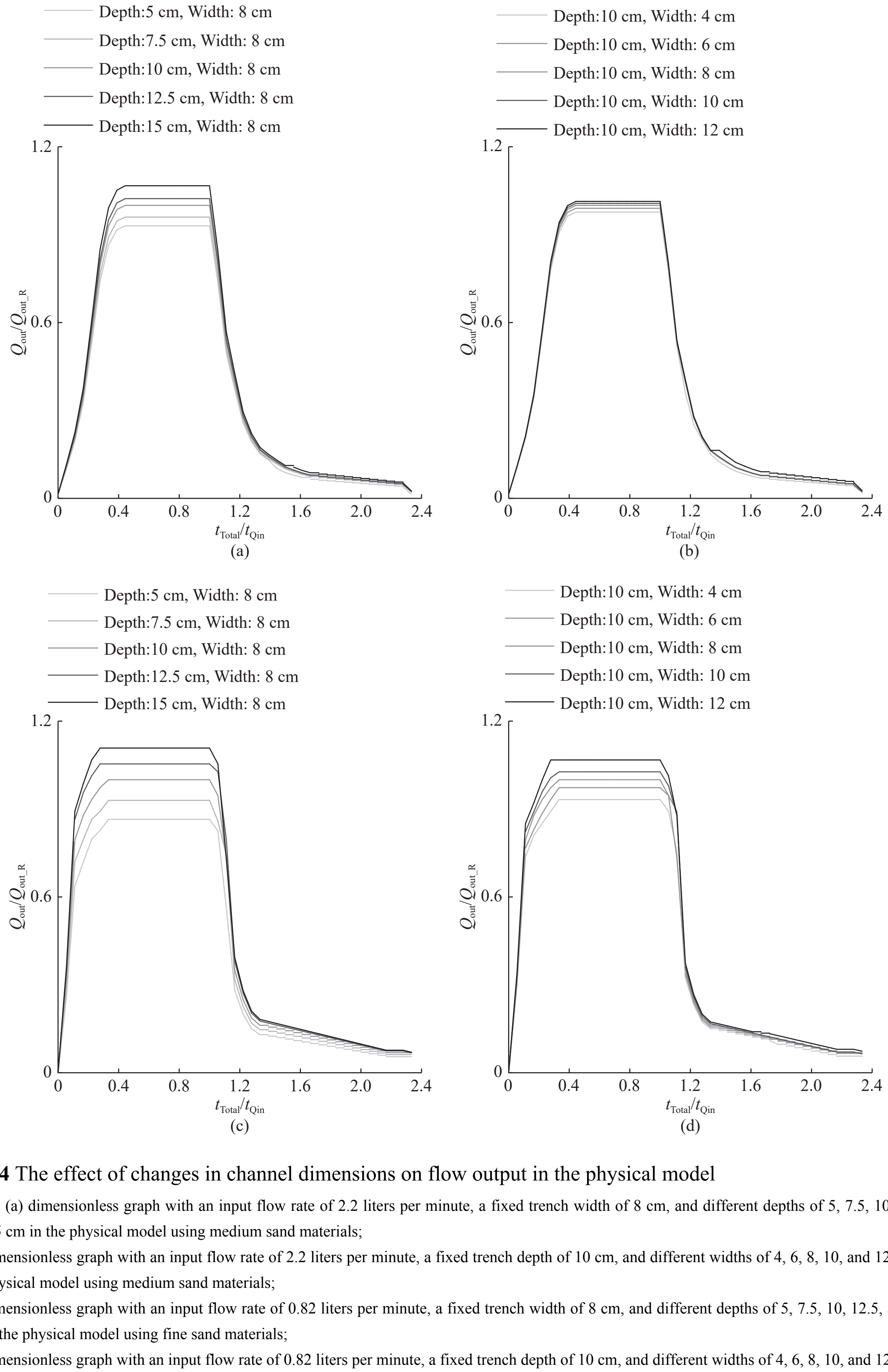

Fig. 4 The effect of changes in channel dimensions on flow output in the physical model

Notes: (a) dimensionless graph with an input flow rate of 2.2 liters per minute, a fixed trench width of 8 cm, and different depths of 5, 7.5, 10, 12.5, and 15 cm in the physical model using medium sand materials;

(b) dimensionless graph with an input flow rate of 2.2 liters per minute, a fixed trench depth of 10 cm, and different widths of 4, 6, 8, 10, and 12 cm in the physical model using medium sand materials;

(c) dimensionless graph with an input flow rate of 0.82 liters per minute, a fixed trench width of 8 cm, and different depths of 5, 7.5, 10, 12.5, and 15 cm in the physical model using fine sand materials;

(d) dimensionless graph with an input flow rate of 0.82 liters per minute, a fixed trench depth of 10 cm, and different widths of 4, 6, 8, 10, and 12 cm in the physical model using fine sand materials.

Where: Q_{out} is output flow rate (m^3/s), D_{50} is average diameter of material particles (m), L is length of the trench, P is the wetted medium (m).

By utilizing the parameters of the physical model, which include the measured output flow rate, depth, width, length of the trench, and aver-

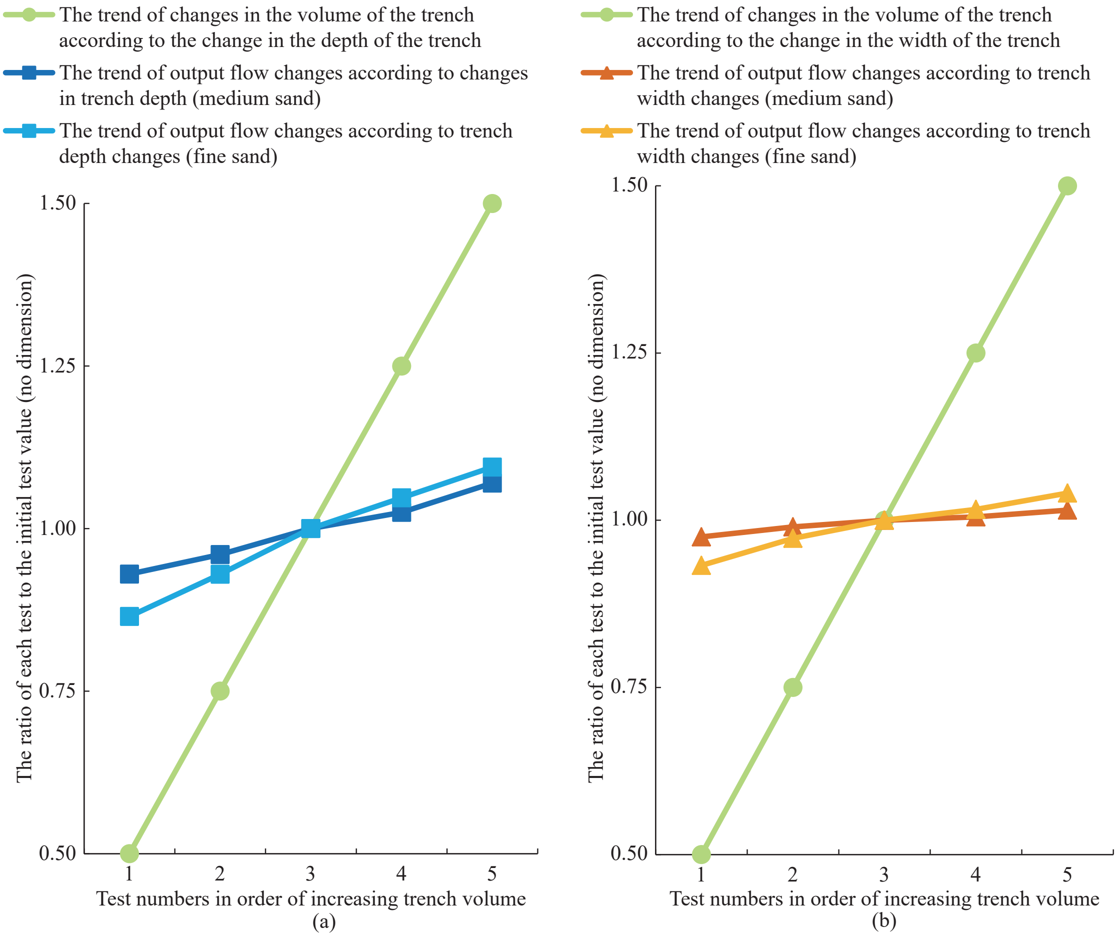

Fig. 5 Examining the changes in the volume of the trench and the changes in the output flow in medium sand and fine sand

(a) according to the changes in the depth of the trench; (b) according to the changes in the width of the trench

age particle diameter, the estimated value of the output flow rate was determined in the above formula.

In this study, to evaluate the presented equation, the Pearson correlation coefficient (r) and the Root Mean Square Error (RMSE) were used. In equations 7 and 8, X_i represents the observed values and Y_i represents the calculated values.

$$r = \frac{\sum_{i=1}^{n}(X_i - \bar{X})(Y_i - \bar{Y})}{\sqrt{\sum_{i=1}^{n}(X_i - \bar{X})^2}\sqrt{\sum_{i=1}^{n}(Y_i - \bar{Y})^2}} \tag{3}$$

$$\mathrm{RMSE} = \sqrt{\frac{\sum_{i=1}^{n}(X_i - Y_i)}{n}} \tag{4}$$

Table 2 and Table 3 display the observed values of Q_{out} and the calculated values of Q_{out} obtained using the provided equation for different trench dimensions for medium sand and fine sand materials, respectively. The Pearson's correlation coefficient (r) and Root Mean Square Error (RMSE) were calculated to assess the performance of the equation. The results indicated that, based on the criteria utilized, the presented equation provides a reliable estimation of Q_{out}. Figs. 7(a) and 7(b) compare the observed values of Q_{out} with the calculated values of Q_{out} from the provided equation, plotted against the 45-degree line for medium sand and fine sand materials, respectively.

2.4 The accuracy of the equation using the field data

Considering that medium sand and fine sand materials were used in the experiments, the average particle dameter (D_{50}) was set within the range of 0.05 millimeters to 2 millimeters in the provided equation.

To assess the accuracy of the equation, it was evaluated using field data obtained from relevant scientific articles. The data from the following studies were utilized to examine the performance of the equation.

(1) Heidarizadeh and Salemi (2014) and Salemi

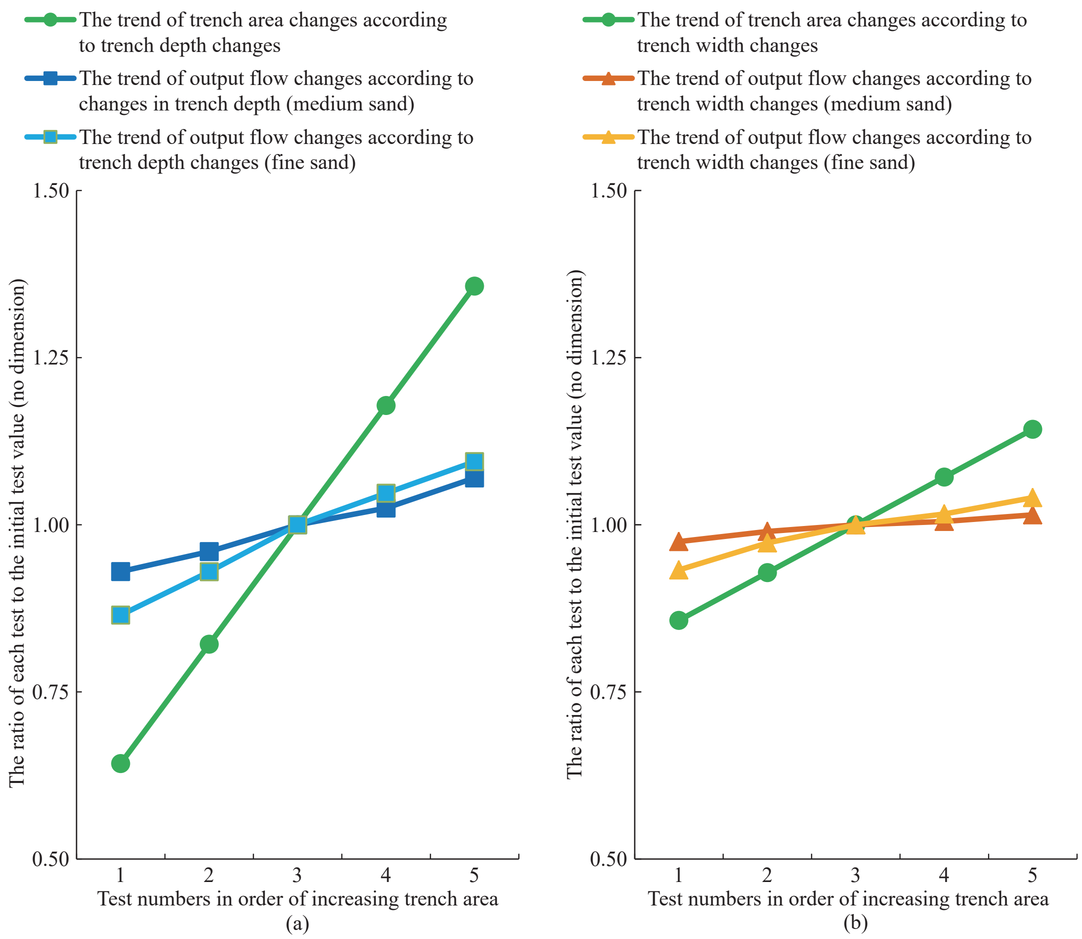

Fig. 6 Examining the changes in the wetted surface of the trench and the changes in the output flow in medium sand and fine sand

(a) according to the changes in trench depth; (b) according to the changes in trench width

Table 2 Comparison of observed values of Q_{out} and calculated values of Q_{out} using the provided equation for different dimensions of the trench in the physical model with medium sand materials

Row	Trench width /cm	Trench depth /cm	Trench length /cm	Q_{out} (Observational) /L/Min	Q_{out} (Computational) /L/Min	Pearson correlation (r)	RMSE
1	8	10	80	1.990	1.969	0.983	0.073
2	4	10	80	1.960	1.863		
3	6	10	80	1.980	1.917		
4	10	10	80	2.010	2.019		
5	12	10	80	2.030	2.066		
6	8	5	80	1.820	1.680		
7	8	7.5	80	1.930	1.835		
8	8	12.5	80	2.050	2.089		
9	8	15	80	2.140	2.198		

and Sepaskhah (2006) conducted studies in the Rodasht area of Isfahan city and the easternmost part of the Zayandehrood River basin. Their objective was to determine the leakage by employing direct measurement method of inlet and outlet discharge in earthen channels used for water transfer in the region (Sharif Abad, Sirian, and Sichi). The hydraulic characteristics of these streams were also measured.

(2) Qabadian and Khalaj (2012) conducted

Table 3 Comparison of observed values of Q_{out} and calculated values of Q_{out} using the provided equation for different dimensions of the trench in the physical model with fine sand materials

Row	Trench width /cm	Trench depth /cm	Trench length /cm	Q_{out} (Observational) /L/Min	Q_{out} (Computational) /L/Min	Pearson correlation (r)	RMSE
1	8	10	80	0.740	0.745	0.992	0.012
2	4	10	80	0.690	0.705		
3	6	10	80	0.720	0.726		
4	10	10	80	0.752	0.764		
5	12	10	80	0.770	0.782		
6	8	5	80	0.640	0.636		
7	8	7.5	80	0.688	0.694		
8	8	12.5	80	0.775	0.791		
9	8	15	80	0.810	0.832		

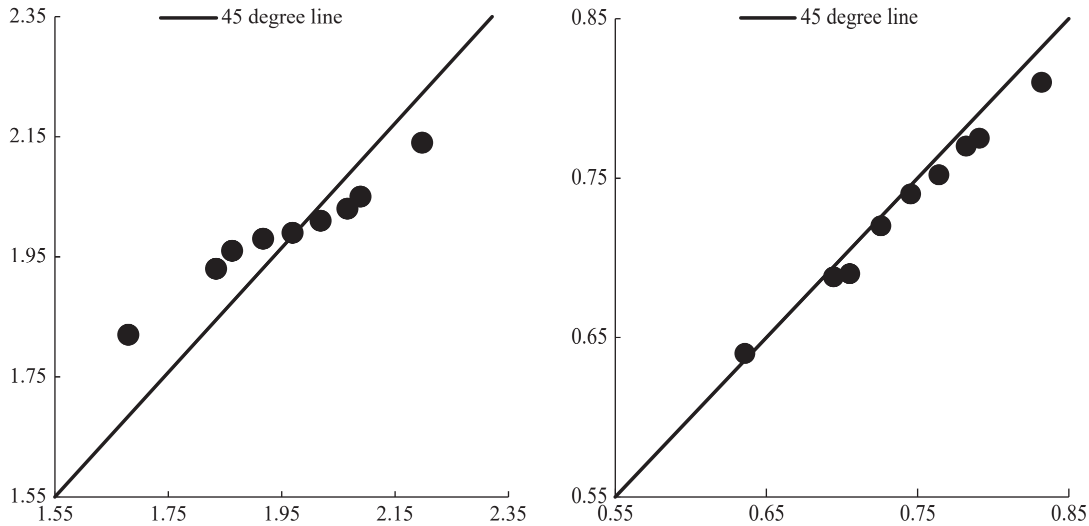

Fig. 7 Comparison of observed values of Q_{out} and calculated values of Q_{out} from the provided equation
(a) for medium sand materials against the 45-degree line; (b) for fine sand materials against the 45-degree line.

research on the losses resulting from water leakage in the Lulam and Sarmast streams in the Nazlu region of Urmia. They used field methods to measure the inflow and outflow flow rates using the OTT model. The hydraulic characteristics of these streams were also measured.

(3) Rostamian and Ebadi Kopaei (2012) employed the method of measuring inflow and outflow to calculate the losses along the Najaf Abad 1 and 2 canals of the Zayandehrud River irrigation network. They selected a specific distance along the canal's length and measured the flow velocity at both the beginning and end of that distance using a sluice gate in various sections. Ultimately, by obtaining the cross-sectional area of the inflow and outflow, they were able to determine their respective discharge. The average hydraulic characteristics of the selected channels were also assessed.

It should be noted that in the above-mentioned articles, the granularity of the soil in the canal bed was determined. The selected channels have an average particle diameter D_{50} within the permissible range of the presentation equation.

In Table 4, the observed values for canal leakage are compared with the calculated values based on the provided equation. Additionally, Fig. 8 displays the observed values for canal leakage alongside the calculated values from equation, along with a 45-degree line.

3 Discussions

3.1 Evaluation and comparison of performance of empirical leakage equa-

Table 4 Compares the observed values of leakage from the channel with its calculated values from the given equation

Row	Channel name	L/m	P/m	D_{50}/m	Q/m^3/d/m^2 Observational	Q/m^3/d/m^2 Computational	Relative error of the main equation/%	Pearson correlation (r)	RMSE
1	Sharifabad	0.35	2.85	0.0003	1.89	1.62	16	0.981	0.381
2	Sirian	0.32	3.14	0.0002	1.78	1.36	30		
3	Cichi	0.96	1.04	0.00015	1.96	1.99	−1.5		
4	Nahr Lulham	0.38	2.6	0.0016	5.58	5.02	11		
5	Nahr Sarmast	0.26	3.88	0.0012	3.87	3.24	19		
6	Garkan 1	0.39	2.59	0.00005	0.55	0.55	0		
7	Garkan 2	0.38	2.61	0.00005	0.59	0.55	7		
8	Najafabad 1	0.76	1.32	0.00015	1.12	1.70	−34		
9	Najafabad 2	0.43	2.34	0.00015	0.95	1.18	−19		

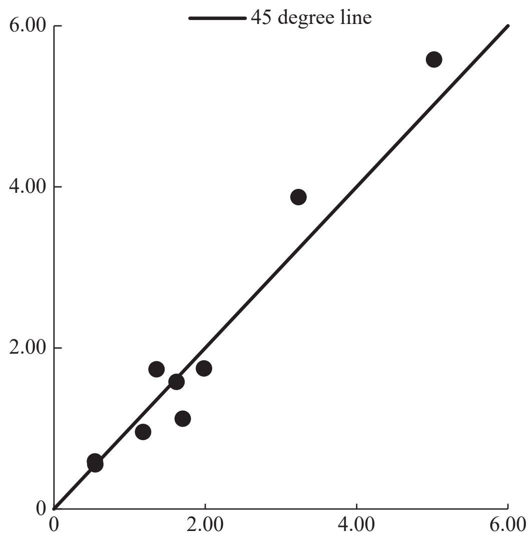

Fig. 8 Comparison of the observed values of leakage from the channel with its calculated values form the equation against the 45-degree line

tions

Tavakoli et al. (2017) noted that an examination of the results obtained from various empirical equations indicates that, except for the Davis-Wilson, Moles-Vers and Yenidomia and India equations, the remaining equations yield estimate of the leakage without under- or over-estimation after adjusting the coefficients. Based on the criteria of RMSE and R^2, the performance of the empirical equations can be ranked as follows after adjusting the coefficients: Moritz, Ingham, Davis-Wilson, Afangenden, Moles-Vers and Yenidomia and India.

In the equation presented in this research, the application of decimal powers to the utilized parameters enables the output estimates to align closely with the observed values. Furthermore, a review of the results from the experimental equations indicates that, aside from the Davis-Wilson, Moles-Verse, Yenidomia and Hindustan equations, the remaining equations, can estimate the leakage amounts without significant discrepancies after correcting the coefficients.

In the study conducted by Rostamian and Abedi Kopaei (2012), the method proposed by Moritz and Ingham demonstrated superior explanatory coefficients when compared to the SEEP/W model. Their results indicated values of 0.373 and 0.183 for Moritz and Ingham, respectively, in contrast to the significantly lower values of 0.093 and 0.067 for the experimental methods of Davis-Wilson, Moles-Vers, and Yenidomia. They reported that the experimental equations were inadequate for accurately simulating leakage amount and performed poorly in the region under study. Although the researchers did not specify the length of the study area for leakage measurement, they highlighted that one reason for the discrepancies between the measured and the modelled leakage values was the use of average hydraulic properties at the inlet and outlet sections in the SEEP/W model. They also noted that the neglect of factors such as vegetation transpiration, root movement, and soil structure degradation. The notably low accuracy of empirical leakage equations before coefficient adjustment, along with the selection of the Moritz and Ingham methods as superior methods to other empirical equations, reflects a similarity between the present study and the findings of Rostamian and Abedi Koupai (2012).

3.2 Inconsistency of the empirical equations of water leakage in different regions and the necessity of their

correction

The studies conducted by Iraq Alavi (1993) on earthen canals under the Zayandeh Rood Dam, propose Misra's experimental method for estimating water leakage from these canals. In contrast, this research introduces the Ingham equation for the Rudasht area. A notable distinction between the two studies is that Iraq Alavi's work focused on the primary and secondary canals, whereas this research investigates the third and fourth-level earthen channels. Consequently, the percentage of vegetation in the irrigation network of Zayandeh Rood is much higher than that in Roodasht.

Additionally, there is a difference in soil composition between the two regions. The Zayandeh Roud network predominantly features silty loam soils, while Rudasht irrigation networks is characterized by clay soils, which are considered heavier. Similarly, Salemi and Sepaskhah (2006) identified the Davis and Wilson equation as the most suitable for estimating water leakage in the Barkhor irrigation network.

The discrepancies among the results from Salemi and Sepaskhah (2006), Iraq Alavi (1993) and Salemi and Sepaskhah (2006) can be attributed to the diversity of soil types and varying vegetation percentages across different regions. Such inconsistencies underscore the necessity of modifying the coefficients of the experimental equations to suit the specific characteristics of each irrigation region.

In the study of Heidarizadeh and Salemi (2014), it was concluded that the theoretical method is preferable to the experimental method for estimating the amount of leakage from channels. Both Ingham's empirical model and Wedernicko's theoretical approach consistently provided lower estimates than the observed values. The authors emphasized that if the variables within a method are properly weighted and incorporated into a relationship, the constant coefficient of that relationship can be accurately estimated across multiple experiments. Otherwise, if these variables are not adequately considered, the coefficients will vary and depend on unconsidered variable.

A comparison between the coefficients from Ingham's experimental model and Wedernik's theoretical method reveals that while the theoretical method can accurately estimate leakage, the maximum value of the coefficient K is 1.45 times greater than its theoretical counterpart. In contrast, the ratio of the maximum to minimum coefficient C in the experimental method is significantly higher, at 22. This finding suggests that the experimental method is more sensitive to the coefficient C than the theoretical method, likely due to the omission of crucial variables. Furthermore, the study indicates that even when correction coefficients are applied to the equations under investigation, these coefficients can vary widely. This variability may further diminish the accuracy of the leakage rate estimations.

3.3 Investigating how soil texture and other factors affect water leakage

The study by Salemi and Sapaskhah (2006) examined lengths in ranging from 216 m to 1,290 m across different channels characterized by light, medium, and heavy soil textures. In contrast, the present study was conducted using a laboratory model that focused on two specific textures: Fine sand and medium sand. The findings from the current study align closely with those reported by Salemi and Sapaskhah (2006).

In the present study, the range of discharge variation for Sharifabad, Sirian, and Sichi earthen channels was measured at 1.36 $m^3/d/m^2$ to 1.99 $m^3/d/m^2$. This is comparable to the figures reported by Salami and Sapazeh (2006), where discharge rate varied from 1.78 $m^3/d/m^2$ to 1.96 $m^3/d/m^2$ during the months of June, July, and August. Given the inherent limitations of the laboratory model, the observed difference in values between the two studies are considered acceptable.

Empirical equations primarily consider the effects of soil texture and hydraulic characteristics of channels; however, other factors can significantly affect the intensity and amount of leakage and water infiltration into the soil. One notable factor is vegetation, as highlighted in the study by Salemi and Sapaskhah (2006). In addition, the percentage of soil particles can also affect infiltration, even when two soils exhibit similar textures according to conventional classification methods. These points highlight the necessity for further investigation into leakage and its influencing factors. Given the diverse regional conditions, variations in soil texture and differing percentages of sand, silt, and clay particles, as well as vegetation, the observed inconsistencies across various studies appear natural.

The coefficients of the leakage equations have been adjusted according to the soil characteristics, vegetation and weather conditions specific to the Rudasht region. However, modifying these coefficients for other regions requires separate plans, as additional factors such as water and soil salinity also play crucial roles in enhancing water permeability and, consequently, the potential for water leakage. This adjustment is particularly important in light of the Ministry of Energy's commitment to modernizing the country's irrigation networks (Salami and Sepaskhah, 2006). In the artificial feeding method presented in this study, the trench structure is designed to prevent vegetation growth, ensuring negligible evaporation. Additonally, the water source used is of acceptable quality. the location of the infiltration trench has also been carefully selected, with the underlying soil exhibiting a relatively specific granularity. In this research, the D_{50} value was determined based on the percentage of sand, silt and clay particles, resulting in a reasonable estimate.

4 Conclusion

As discussed in the previous sections, several factors, including vegetation, weather conditions, and evaporation influenced by wind and temperature, can impact the accuracy of leakage estimation. However, the proposed method minimizes these errors by using trenches with specific characteristics. The incorporation of coarse-grained materials in these trenches while not only stabilizes their structure but also enhance hydraulic performance, facilitating efficient water flow. Because the leaking water doesn't come into contact with the air, evaporation is negligible, and the lack of air and light inside the trench prevents plant growth. Furthermore, the developments of biofilm on these materials contribute to the purification of the used water. In addition, this method offers the advantages of controllability over the amount of fed water, the ability to adjust trench depth according to the soil layers, and the prevention of canal wall collapse, all of which significantly reduce estimation errors.

After conducting a series of controlled experiments and statistical analysis of the data, a new empirical equation was developed to describe the behavior of the proposed method. The results indicated that changes in trench depth have a more significant impact on increasing infiltration compared to the changes in trench width. Additionally, variation in the volume of the trench or the wetted surface area of the trench demonstrate a greater effect on output in fine sand textures than in medium sand.

In the relationship presented in Equation 6, D_{50} is utilized to determine the type of bed soil. By preparing the granulation curve of each soil, an accurate value of D_{50} can be obtained, highlighting the superiority of this equation over the aforementioned experimental equations.

As previously explained, the range of D_{50} values considered in this study is between 0.05 mm and 2 mm, resulting in a ratio of 40 times between the highest and lowest values in this range. This substantial variation can lead to rapid changes in the solution for leakage causing the output to diverge significantly from reality. The decimal power assigned to the D_{50} parameter in Equation 2 ensures that its impact on Q_{out} (leakage from the channel) is proportional.

Regarding the wetted medium (P), observations from the experiments revealed that the ratio of change in Q_{out} (leakage from the channel) is inconsistent with changes in the wetted area. For instance, when comparing row 9 with row 6 of Table 2, the wetted area has increased by 77%, yet Q_{out} (leakage from the channel) only increased by 17%. This discrepancy highlights the significance of the decimal power assigned to the parameter P, which determines its influence on the leakage rate. The proposed method for estimating leakage in earthen canals is based on an empirical equation derived from controlled experiments. This equation incorporates factors such as soil type, trench dimensions, and wetted surface area to accurately predict leakage rates.

A comparative analysis of observed data from nine Iranian earthen canals and calculated values using the proposed equation revealed a mean relative error of 15% between the two datasets. Additionally, a Pearson correlation coefficient of 0.981 and an RMSE of 0.381 were determined, collectively indicating the equation's robust performance. The parameters considered in the presented equation enhance its application across various regions. Given the satisfactory results obtained, this equation can provide a reliable initial estimate of the leakage rate, ultimately reducing costs and saving time.

References

Afzali SH, Abedini MJ, Monajemi P. 2009. Simulation of flow in porous media using coupled pressurized-free surface interconnected conduit network 1- network analysis. Iran-Water Resources Research, 5(2): 62–70. (in Persian)

Ali H. 2011. Practices of irrigation & on-farm water management. Springer Science & Business Media, New York, USA, 546. DOI：10.1007/978-1-4419-7637-6.

Bagarello V, Sferlazza S, Sgroi A. 2009. Testing laboratory methods to determine the anisotropy of saturated hydraulic conductivity in a sandy–loam soil. Geoderma, 154(1): 52–58. DOI：10.1016/j.geoderma.2009.09.012.

Beckwith C, Baird A, Heathwaite AL. 2003. Anisotropy and depth-related heterogeneity of hydraulic conductivity in a bog peat. I: Laboratory measurements. Hydrological Processes, 17(1): 89–101. DOI：10.1002/hyp.1116.

Cui YL, Li YH, Mao Z, et al. 2004. Strategies for improving the water supply system in HCID, upper reaches of the Yellow River Basin, China. Agricultural Engineering International: The CIGR Journal of Scientific Research and Development. Manuscript LW 02 005.

Detay M, L Bersillon J. 1996. La réalimentation artificielle des nappes profondes: Faisabilité et conséquences. La Houille Blanche, Revue Internationale De l'eau, 4: 57–61. (in French) DOI：10.1051/lhb/1996040.

El Mansouri B, El Mezouary L. 2015. Enhancement of groundwater potential by aquifer artificial recharge techniques: An adaptation to climate change. Proceedings of the International Association of Hydrological Sciences, 366: 155−156. DOI：10.5194/piahs-366-155-2015.

Foreman TL. 2014. Managed Aquifer Recharge (MAR) and design and construction of hydraulic barriers against seawater intrusion: The California case. Boletín Geológico y Minero, 125 (2): 133–142.

Heidarizadeh M, Salemi HR. 2014. Comparison of Wedernikow theoretical method with Ingham empirical method in estimation of seepage from earth channels in Roodasht Region of Isfahan. Agricultural Water Research Journal, 28(4): 703−712. DOI：10.22092/jwra.2015.100825.

Hiscock KM, Balashova N, Cooper RJ, et al. 2024. Developing Managed Aquifer Recharge (MAR) to augment irrigation water resources in the sand and gravel (Crag) aquifer of coastal Suffolk, UK. Journal of Environmental Management, 35: 119639. DOI：10.1016/j.jenvman.2023.119639.

Iraq Alavi S. 1993. Management of Zayandeh Rud water distribution based on the estimation of water conveyance efficiency in downstream canals. Isfahan University of Technology, Master's Thesis in Irrigation and Drainage, Department of Irrigation and Drainage, 150.

Karim I, Abd Ali AM. 2018. Artificial recharge of groundwater by injection wells: A case study. International Journal of Science Engineering and Technology, 6(1): 6193–6196.

Lhassan MS, Bouabid EL M, Badr B, et al. 2019. Improvement of groundwater resources potential by artificial recharge technique: A case study of Charf El Akab aquifer in the Tangier region, Morocco. Journal of Groundwater Science and Engineering, 7(3): 224−236. DOI：10.19637/j.cnki.2305-7068.2019.03.003shu.

Li HX, Han SB, Wu X, et al. 2021. Distribution, characteristics and influencing factors of fresh groundwater resources in the Loess Plateau, China. China Geology, 4(3): 509−526. DOI：10.31035/cg2021057.

Moghazi HEM, Ismail ES. 1997. A study of losses from field channels under arid region conditions. Irrigation Science, 17(3): 105−110. DOI：10.1007/s002710050028.

Murillo Díaz JM. 2004. Recarga de acuíferos. Evaluación y análisis de condicionantes técnicos y económicos. Acuífero aluvial del Bajo Guadalquivir. Minas. (in Spanish)

Nan T, Shao JL, Cui YL. 2016. Column test-based features analysis of clogging in artificial recharge of groundwater in Beijing. Journal of Groundwater Science and Engineering, 4(2): 88−95. DOI：10.26599/JGSE.2016.9280011.

Nouri Mohammadieh M, Sohrabi T, Rahimi H. 2010. Evaluation of empirical equations of seepage estimation from earthen canals (Case study: Ghazvin Plain). Iranian Water Research Journal, 4(2): 125–128.

Pishro F, Morteza Bakhtiari M, Shahni Karamzadeh N. 2017. Laboratory investigation of soil mechanical indices on anisotropic permeability of non-uniform coarse-grained materials: With emphasis on grain size, shape factor and density. Journal of Advanced Applied Geology, Shahid Chamran University of Ahvaz, 7(2): 57–64. (In Persian) DOI：10.22055/aag.2017.21062.1665.

Pyne RDG. 2005. Aquifer storage and recovery: A guide to groundwater recharge through wells

Edition. ISBN 0-9774337-090000.

Qabadian R, Khalaj M. 2012. Numerical estimating of earth channel seepage in Nzloo Area of Uromye Province and correction of empirical relation constant coefficient. Journal of Water and Soil (Agricultural Sciences and Industries), 26(1): 193−202. DOI：10.22067/jsw.v0i0.13648.

Rognon P. 2000. Comment développer la recharge artificielle des nappes en régions sèches. Sécheresse, 11(4): 289−296. (in French)

Rostamian R, Abedi Koupai J. 2012. Assessment of SEEP/W Model to estimate seepage from earth canals (Case study: Irrigation Network of Downstream Zayandehrud). JWSS-Isfahan University of Technology, 15 (58) : 13–22.

Salemi HR, Sepaskhah AR. 2006. Estimation of canal seepage loss in Rudasht Region of Isfahan. Journal of Agricultural and Natural Resources Sciences, 10(2): 42–29.

Scanlon B, Keese K, Flint A, et al. 2006. Global synthesis of groundwater recharge in semiarid and arid regions. Hydrological Processes, 20(15): 3335–3370. DOI：10.1002/hyp.6335.

Sebbar A. 2013. Etude de la variabilité et de l'évolution de la pluviométrie au Maroc (1935-2005): Réactualisation de la carte des précipitations. Thèse national, Université Hassan II Mohammedia-Casablanca, Maroc. (in French) DOI：10.13140/2.1.1206.6084.

Senent-Alonso M. 1984. Problems of the artificial recharge of aquifers. Spanish achievements and their possibilities in the southeast of Spain. Doctoral Thesis, University Polytechnic of Madrid.

Tavakoli E, Ghorbani B, Samadi Borujeni H, et al. 2017. Modifying empirical equations of seepage estimation using dimensional analysis (Boldaji earth canal, Chaharmahal and Bakhtiari province). Water and Soil Conservation Journal, 6(2): 105–119.

Zhang G, Lu N, Liu J, et al. 2015. River leakage ratio and leakage amount in the Qaidam Basin. Geological Bulletin of China, 34(11): 2083−2086. (in Chinese)